Egyptian Journal of Chemistry
http://ejchem.journals.ekb.eg/

Synthesis Of Mono and Bimetallic Metal-Organic Frameworks For Photocatalytic Degradation Of Bis-phenol A Under Natural Solar Irradiation

Aya E. Abdel Razek, [a] Nasser Y. Mostafa, [b] Mohamed A. M. Abdel Reheim, [a] Metwally Madkour, [a] Ahmed M. Tolba. [a,*]

[a]*Chemistry Department, Faculty of Science, Arish University, Al-Arish 45511, Egypt.*

[b]*Chemistry Department, Faculty of Science, Suez Canal University, Ismailia, Egypt.*

Abstract

Herein, a facile synthesis of new photocatalysts of metal-organic frameworks (MOFs) using terephthalic acid as a linker and Ni and Ni/Cu as mono and bimetallic centers has been prepared. Further, the MOF photocatalysts were characterized by X-ray powder diffraction, scanning electron microscopy, and X-ray photoelectron spectroscopy and Molecular absorption spectroscopy techniques. Their photocatalytic activities toward Bis-phenol A photodegradation have been tested under natural solar irradiation. The bimetallic Cu/Ni-MOF photocatalyst demonstrated a superior photodegradation efficiency (77.4 %) after 120 min compared to 44.5 % for Ni-MOF. This is due to the impact of Cu introduction to the Ni-MOF matrix which reduced the band gap energy value, 2.87 eV and 2.22 eV for Ni-MOF and Cu/Ni-MOF, respectively. The obtained results revealed the potential of such photocatalysts to efficiently degrade wastewater pollutants under natural solar irradiation.

Keywords: Metal-organic frameworks; Bimetallic MOFs; solar irradiation; photocatalysis; nanoparticles.

1. Introduction

The development of effective and sustainable wastewater treatment technology is required due to the growing concern over environmental degradation and water scarcity [1]. Conventional techniques, although efficient, may produce secondary contaminants or need a significant amount of energy. Photocatalysis is a potential substitute for wastewater treatment that uses light to initiate chemical processes. Using sunlight as the energy source, solar photocatalysis offers an especially appealing method for breaking down organic contaminants in wastewater [2, 3].

Metal-organic frameworks (MOFs) have become an innovative class of photocatalytic materials because of their extremely adjustable architectures [4]. The building blocks of these porous crystalline materials are metal ions or clusters joined by organic linkers [5]. Because of their modular nature, MOFs can be modified to target contaminants. The organic linkers and integrated metal centers have a major impact on surface reactivity, charge separation, and light absorption—all essential elements of effective photocatalytic degradation [6].

The utilization of MOF modified visible active photocatalysts has been disclosed. A hydrothermal method was utilized to successfully prepare cobalt/nickel-based metal-organic frameworks (Co/Ni-MOFs) modified bismuth oxyiodine (BiOI) composite (Co/Ni-MOFs@BiOI) as a new visible light active photocatalyst for the disintegration of methylene blue dye (MB) in water solutions [7]. Also, using a simple solvothermal technique, CdS nanoparticles were hybridized with titanium metal-organic framework (MOF) and graphitic carbon nitride (g-C3N4) sheets for the visible light-induced photocatalytic degradation of rhodamine B dye [8].

This research is focused on the utilization of the solar photocatalytic activity of MOFs. We explore the fundamental principles governing their photocatalytic behavior and investigate strategies for optimizing their performance. Our focus lies on preparation of

*Corresponding author e-mail: atolba@aru.edu.eg.; (Ahmed M. Tolba).
Receive Date: 10 June 2024, Revise Date: 23 June 2024, Accept Date: 10 July 2024
DOI: 10.21608/ejchem.2024.296325.9838

Ni and Ni/Cu as mono and bimetallic MOF using terephthalic acid as a linker. The prepared MOFs structures were characterized then we aim to elucidate the relationship between MOF structure and photocatalytic activity vis Bisphenol A solar photodegradation. This research contributes to the advancement of MOF-based photocatalysis, paving the way for their practical applications in solar energy conversion and environmental remediation.

Experimental:

Preparation of Ni-MOF.

Ni-MOF was synthesized hydrothermally from Terephthalic acid and NiCl2·6H2O with a little modification. and the schematic diagram is shown in **Fig. 1**. Typically, with a molar ratio of 1:1 terephthalic acid (1.66 g) was dissolved in DMF (75 ml) under continuous stirring. Another solution was prepared, NiCl2·6H2O (1.3 g) was dissolved in a solvent mixture of Ethanol (25 ml) and DI water (5.0 ml) with stirring. To create a homogeneous solution, both solutions were combined and stirred continuously for one hour. The resulting mixture was then transferred to an autoclave lined with Teflon and baked for three days at 105°C. After letting the solution drop to room temperature for the whole night, it was filtered and repeatedly washed with distilled water, DMF, and ethanol. Before being utilized, the resultant light green crystals were dried for 12 hours at 60 °C in a vacuum atmosphere.

Preparation of Bimetallic Cu/Ni-MOF.

A facile hydrothermal method was used for the synthesis of Cu/Ni-MOF with a little modification. The schematic diagram is shown in **Fig. 2**. $NiCl_2{\cdot}6H_2O$ (0.65 gm) and $Cu(CH_3COO)_2$ (0.99 gm) were mixed in the molar ratio of 0.5 : 0.5 and dissolved a solvent mixture of Ethanol (40 ml) and DI water (10 ml) with stirring. Subsequently, 1.66 gm of the terephthalic acid ligand was dissolved in DMF (75 ml) under continuous stirring. To obtain a homogenous solution, Both the solutions were mixed under continuous stirring for 1.0 hour and then collected into a Teflon-lined autoclave and kept at 105 °C for a period of 3 days. After letting the solution drop to room temperature for the whole night, it was filtered and repeatedly washed with distilled water, DMF, and ethanol. Before being used, the resultant blue-green crystals were dried for 12 hours at 60 °C in a vacuum atmosphere.

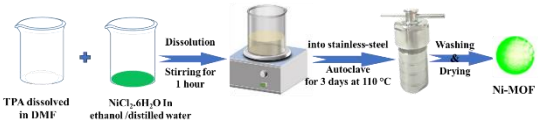

Fig. 1. Schematic preparation of Ni-MOF.

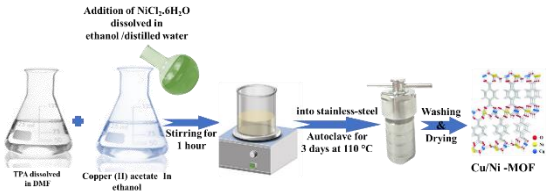

Fig. 2. Schematic preparation of Cu/Ni-MOF.

Characterization of prepared compounds

The UV-Vis spectrophotometer was used to assess the absorption characteristics of the substance. The crystallite size and crystal structure of the nanoparticles were investigated using the X-ray powder diffractometer (XRD). The C1s peak at 284.6 eV served as the reference point for the XPS spectrometer, which was used to perform X-ray photoelectron spectroscopy (XPS). Furthermore, a JSM-7100F (JEOL) was used to study field emission scanning electron microscopy (FE-SEM) findings.

Photocatalytic activity

The produced NPs' photocatalytic activity was assessed for photodegradation of Bisphenol A (20 ppm) in natural sunlight as a pollutant model. In batch experiments, Bisphenol A model polluted water (Bisphenol A: 0.1 g/L) were stirred for 20 minutes to attain adsorption-desorption equilibrium before moving on to photodegradation experiments. On days when the sky was clear and there were no clouds, the natural sun radiation was measured between December 10 and January 2024. On the roof of the building of faculty of Science, Arish University.
Using a digital illumination meter, the incoming average solar energy was determined to be around 83.400 flux (659 W/m^2) (INS, DX-200). Bisphenol A solutions in 5.0 ml aliquots were collected and subjected to spectrophotometric analysis every 20 minutes. To separate the nanoparticles from the fluid, the suspension was centrifuged each time. The kinetics of Bis-Phenol A photodegradation were investigated by measuring absorption spectra (at λmax = 278 nm) every 20 minutes.

Results and Discussion

Morphological studies

Using scanning electron microscopy (SEM), the morphology of Ni-MOF and Cu/Ni-MOF was examined, as illustrated in Fig. 1. It illustrates that while the characteristics differ, both samples are made of microspheres, which are made of several interconnected nanoribbons. Cu ions are seen to cause the sheet-shaped nanoribbons of Cu/Ni- MOF to become broader and exhibit a more regular arrangement.

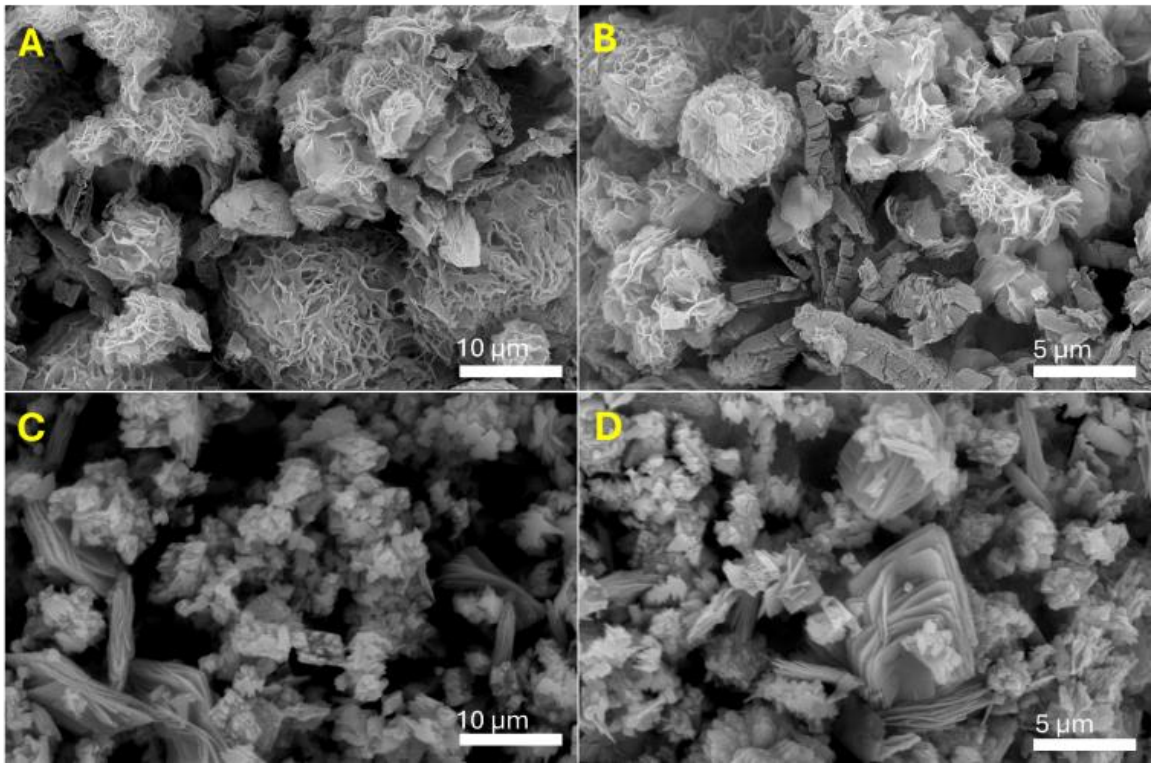

Fig.3. FE-SEM of Ni-MOF (A, B) and Cu/Ni-MOF (C, D).

Structural studies

For bulk structural characterization, the XRD patterns of the photocatalysts are shown in **Fig. 2**. The diffraction peaks of as-prepared Ni-MOF and Cu/Ni-MOF. XRD pattern of Ni-MOF shows the primary signature diffraction peaks at 2θ values of (11.86◦, 15.8◦, 18.4◦, 24.03◦, 28.4◦, 31.8◦ and 40.4◦) correspond to (010), (10^{-}1), (1^{-}11), (2^{-}11), (002), (20^{-}2) and (4^{-}11) crystal planes [9]. The powder XRD pattern of Cu/Ni-MOF showed diffraction peaks at 2θ values of 19.7°, 21.7°, 22.7°, 27.8°, 30.2°, 32.9°, 33.6°, 35.7°, 37.7°, and 44.2°. Also, from XRD pattern of Cu/Ni-MOF, it showed (1 1 1) and (2 0 0) planes at 44.2, 49.3° and 52.3 which is an indicative for the polycrystalline structure Ni and Cu and confirmed the interaction of the bimetallic centers [10, 11].

The Scherrer equation was utilized to determine the average crystallite sizes of each nanoparticle by taking the whole width at half-maximum of the most intense peak profile:

$$D = K\lambda / \beta \cos\theta \qquad [1]$$

Where D is the size of the crystallite, K is the Scherrer constant, which is equal to 0.9, the X-ray wavelength is λ = 0.1541 nm, the full width half maximum (FWHM) is β, and the diffraction angle is θ. The crystallite size results were found to be 10.61 and 9.83 nm for Ni-MOF and Cu/Ni-MOF respectively.

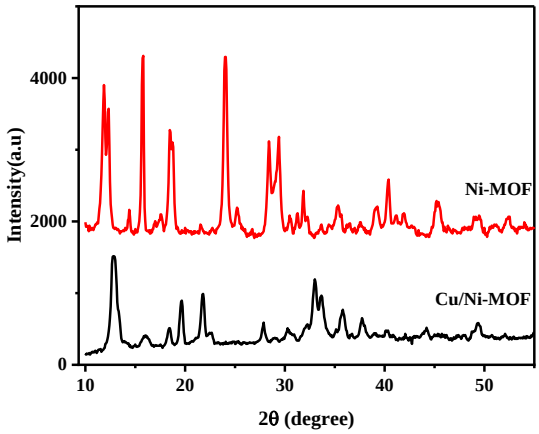

Fig.4. XRD pattern of the as-synthesized Ni-MOF and Cu/Ni-MOF.

For surface structural characterization, In **Fig. 5.** XPS spectra of Ni-MOF and Cu/Ni-MOF contains Ni, Cu, C and O elements. It Shows deconvolution of the Ni 2p1/2 band into two spectral bands at 873.92 eV and 875.99 eV. Also, the Ni 2p3/ 2 band was deconvoluted into two spectral bands at 856.16 eV and 858.11 eV. The two other shake-up satellite peaks are situated at 863.10 eV and 881.20eV. respectively, suggesting that Ni ions are bivalent [12, 13]. Additionally, spectrum contains Cu 2p ,which shows Two significant peaks: one at 953.6 eV, identified as Cu2p1/2, and another at 933.8 eV, identified as Cu2p3/2. Cu2p3/2 produced two further peaks with binding energies of 941.4 and 943.8 eV, respectively, and Cu2p1/2 produced additional peaks

at 962.6 eV. These are satellite peaks, indicating that Cu is present in the Cu^{2+} oxidation state [14, 15]. Also, XPS spectrum of O1s displayed the two discrete spectra C–O/C=O (533.66 eV) and M–O–C/H (531.71 eV) [16] (M=metal) that were assigned to lattice and surface oxygen, respectively [13]. Also, XPS spectrum of the C1s peak indicates a deconvolution into three peaks. The reference C1s peak was linked to the peak at 284.6 eV, while the aryl carbon from the benzene ring and the carboxylate carbon in O-C=O were responsible for the other two peaks, which are located at 285.87 eV and 288.93 eV, respectively [17], strongly suggesting the existence of terephthalic acid [18].

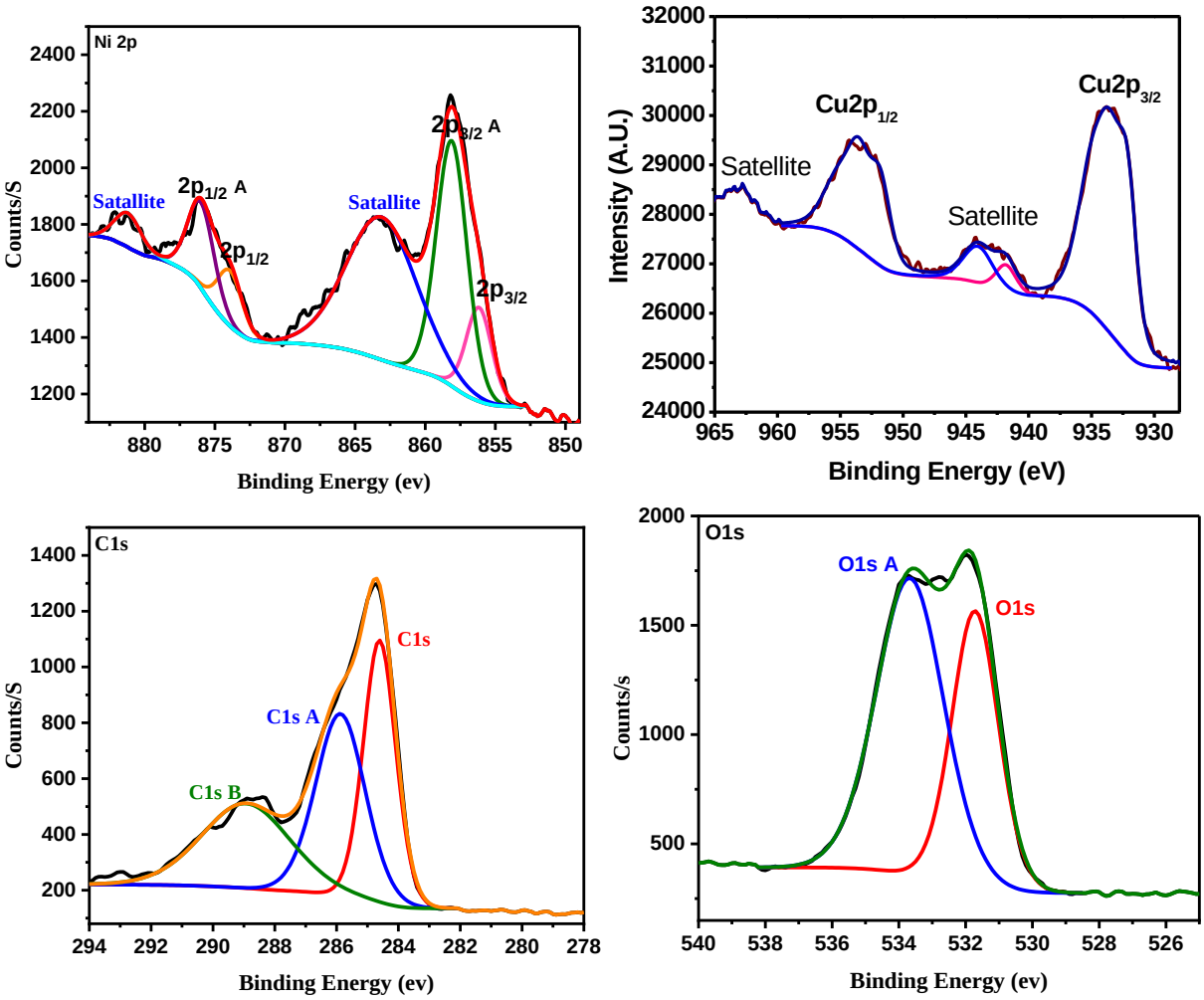

Fig.5. XPS spectra of Ni 2p, Cu 2p, C 1s and O 1s scan spectrum of Ni-MOF and Cu/Ni-MOF.

Optoelectronic properties

Using UV-vis absorption spectroscopy, the catalyst's capacity to absorb light was evaluated [19]. The results of the UV-vis spectra of the as-prepared Ni-MOF and Cu/Ni-MOF are pointed in **Fig. 6.** The UV-Vis spectrum of Ni-MOF shows an absorption peak at 432 nm. The electron transfer $\pi \rightarrow \pi^*$ in terephthalic acid may have contributed to the absorption band at the UV region. The visible absorption band ought to be connected to the electron transport in orbital 3d [20]. The UV-vis spectrum of Cu/Ni-MOF shows an absorption peak at 558.5 nm.
The band gap energy (Eg) of Ni-MOF and Cu/Ni-MOF can be calculated using Tauc plot method:[21] $(\alpha h\nu)2 = B(h\nu - Eg)$, where B, α and ν are proportionality constant, absorption coefficient and light frequency, respectively. The $(\alpha h\nu)^2$ versus hν curves for Ni-MOF and Cu/Ni-MOF are shown in **Fig. 7**. The band gap energies were estimated to be 2.87 eV and 2.22 eV for Ni-MOF and Cu/Ni-MOF samples, respectively.

Photocatalytic measurements

The photocatalytic destruction of bisphenol A by solar radiation was investigated using Ni-MOF and Cu/Ni-MOF photocatalysts. First, a control experiment called photolysis was carried out, in which Bisphenol A was exposed to the same solar radiation conditions without the use of

photocatalysts. Only 5.0% of the bisphenol A was degraded, according to the photodegradation data, which also revealed a modest drop in the concentration of bisphenol A. Representative UV-vis absorption spectra of aqueous solutions of Bisphenol A irradiated under natural sun light after each 20 minutes in the presence of Ni-MOF, Cu/Ni-MOF photocatalysts were recorded. The photocatalytic activities of the Ni-MOF and Cu/Ni-MOF photocatalysts under natural sunlight irradiation were assessed for Bisphenol A photodegradation.

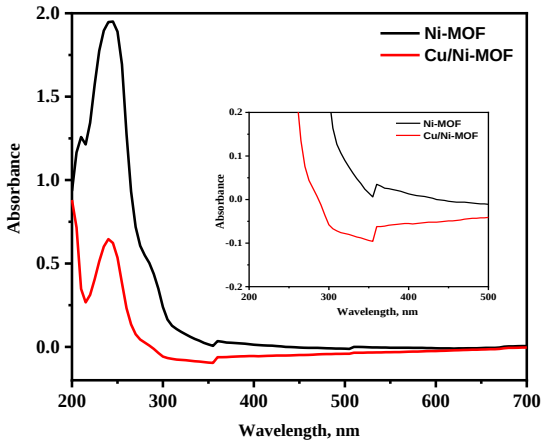

Fig.6. UV-vis spectra of Ni-MOF and Cu/Ni-MOF nanoparticles.

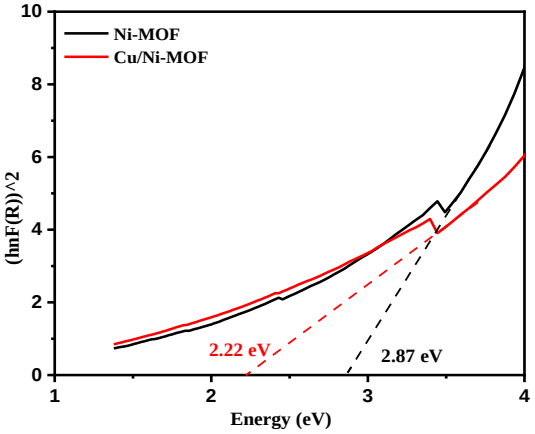

Fig.7. The Tauc plot of (αhν)2 versus hν for Ni-MOF and Cu/Ni-MOF nanoparticles.

By comparing the absorbance variations at λmax = 278 nm versus different irradiation periods, the photocatalytic decomposition of bisphenol A was observed.

The degradation rate constant for the photodegradation reaction was found using equation 2, which describes the pseudo-first-order reaction kinetics for the photocatalytic process.:

$$Ln(C_0/C) = -kt \qquad [2]$$

Where k is the apparent first-order rate constant, C_0 is the starting concentration, and C is the concentration at each time. The slope of a straight-line plotting Ln C_0/C against time, as determined by linear regression, equals the apparent first-order rate constant, k. For Ni-MOF and Cu/Ni-MOF photocatalysts, the estimated rates of bisphenol A photodegradation were 0.005 and 0.029 min^{-1}, respectively (Fig. 8). The degradation efficiency (E%) was computed by using the following formula:

$$E\,\% = 100 \times \left[\frac{C_0 - C}{C_0}\right] \qquad [3]$$

After 120 minutes, an enhanced photodegradation efficiency was noted for Cu/Ni-MOF, which is more than half the value of bare Ni-MOF (Fig. 9). In the presence of Ni-MOF and Cu/Ni-MOF photocatalysts, respectively, the photocatalytic degradation of bisphenol A was determined to be 44.5% and 77.4%.

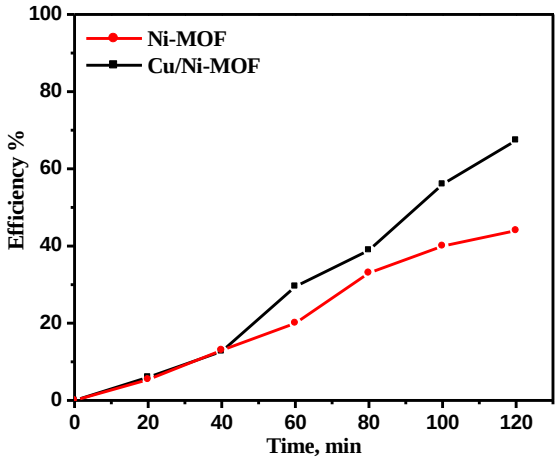

Fig.8. Bisphenol A solar photodegradation efficiency at varied degradation times when irradiated with Ni-MOF and Cu/Ni-MOF.

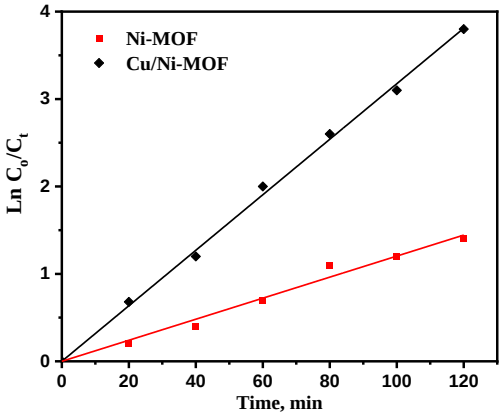

Fig.9. Bisphenol A solar photodegradation rate at varied degradation times when irradiated with Ni-MOF and Cu/Ni-MOF.

2. Conclusion

Ni and Ni/Cu as mono and bimetallic metal-organic frameworks (MOFs) were successfully synthesized via a simple and modified hydrothermal

method. The obtained narrow band gaps 2.87 eV and 2.22 eV for Ni-MOF and Cu/Ni-MOF, respectively made them promising photocatalysts for the photodegradation of Bisphenol A from wastewater under solar irradiation. The bimetallic Cu/Ni-MOF photocatalyst demonstrated a superior photodegradation efficiency (77.4 %) after 120 min compared to 44.5 % for Ni-MOF.

3. References

[1] R. Sangamnere, T. Misra, H. Bherwani, A. Kapley, R. Kumar, A critical review of conventional and emerging wastewater treatment technologies, Sustainable Water Resources Management, 9 (2023) 58.

[2] X. Yang, D. Wang, Photocatalysis: From Fundamental Principles to Materials and Applications, ACS Applied Energy Materials, 1 (2018) 6657-6693.

[3] X. Sun, S. Jiang, H. Huang, H. Li, B. Jia, T. Ma, Solar Energy Catalysis, Angewandte Chemie International Edition, 61 (2022) e202204880.

[4] A. Dhakshinamoorthy, A.M. Asiri, H. García, Metal–Organic Frameworks as Multifunctional Solid Catalysts, Trends in Chemistry, 2 (2020) 454-466.

[5] J.-L. Wang, C. Wang, W. Lin, Metal–Organic Frameworks for Light Harvesting and Photocatalysis, ACS Catalysis, 2 (2012) 2630-2640.

[6] Y. Liu, S. Huang, X. Huang, D. Ma, Enhanced photocatalysis of metal/covalent organic frameworks by plasmonic nanoparticles and homo/hetero-junctions, Materials Horizons, 11 (2024) 1611-1637.

[7] L. Chen, X. Ren, N.S. Alharbi, C. Chen, Fabrication of a novel Co/Ni-MOFs@BiOI composite with boosting photocatalytic degradation of methylene blue under visible light, Journal of Environmental Chemical Engineering, 9 (2021) 106194.

[8] Y. Chen, B. Zhai, Y. Liang, Y. Li, J. Li, Preparation of CdS/ g-C3N4/ MOF composite with enhanced visible-light photocatalytic activity for dye degradation, Journal of Solid State Chemistry, 274 (2019) 32-39.

[9] S. Gao, Y. Sui, F. Wei, J. Qi, Q. Meng, Y. He, Facile synthesis of cuboid Ni-MOF for high-performance supercapacitors, Journal of Materials Science, 53 (2018) 6807-6818.

[10] S. Gopi, A.M. Al-Mohaimeed, W.A. Al-onazi, M. Soliman Elshikh, K. Yun, Metal organic framework-derived Ni-Cu bimetallic electrocatalyst for efficient oxygen evolution reaction, Journal of King Saud University - Science, 33 (2021) 101379.

[11] M. Abbasi, T. Noor, N. Iqbal, N. Zaman, Electrocatalytic study of cu/Ni MOF and its g-C3N4 composites for methanol oxidation reaction, International Journal of Energy Research, 46 (2022) 13915-13930.

[12] F.A. El-Saied, M.M.E. Shakdofa, M.S. Ali, R.M.W. Faried, A. El-Asmy, M. Madkour, Novel thiosemicarbazone complexes as single coordinated precursors for noble metal modified nickel oxide nanophotocatalysts, Journal of Physics and Chemistry of Solids, 157 (2021) 110218.

[13] M. Ravipati, S. Badhulika, Solvothermal synthesis of hybrid nanoarchitectonics nickel-metal organic framework modified nickel foam as a bifunctional electrocatalyst for direct urea and nitrate fuel cell, Advanced Powder Technology, 34 (2023).

[14] M. Madkour, CuxO thin films via ultrasonic spray pyrolysis as efficient solar photocatalysts: Single source polymeric coordinated precursor, Colloid and Interface Science Communications, 44 (2021) 100497.

[15] E. Al-Hetlani, M.O. Amin, M. Madkour, B. D'Cruz, Forensic determination of pesticides in human serum using metal ferrites nanoparticles and SALDI-MS, Talanta, 221 (2021) 121556.

[16] J. Zhang, C. Xu, J. Li, H. Lu, S. Zhang, C. Wang, Controlled synthesis of Cu-/Ni-based 1D c-MOFs and their application in near-linear temperature sensing, Vacuum, 211 (2023).

[17] C. Meng, Y. Cao, Y. Luo, F. Zhang, Q. Kong, A.A. Alshehri, K.A. Alzahrani, T. Li, Q. Liu, X. Sun, A Ni-MOF nanosheet array for efficient oxygen evolution electrocatalysis in alkaline media, Inorganic Chemistry Frontiers, 8 (2021) 3007-3011.

[18] W. Lu, X. Wu, Ni-MOF nanosheet arrays: efficient non-noble-metal electrocatalysts for non-enzymatic monosaccharide sensing, New Journal of Chemistry, 42 (2018) 3180-3183.

[19] Z. Qian, Z.J. Wang, K.A.I. Zhang, Covalent Triazine Frameworks as Emerging Heterogeneous Photocatalysts, Chemistry of Materials, 33 (2021) 1909-1926.

[20] H. Nishimura, T. Okazaki, Y. Tanaka, K. Nakatani, M. Hara, A. Matsumori, S. Sasayama, A. Mizoguchi, H. Hiai, N. Minato, T. Honjo, Autoimmune dilated cardiomyopathy in PD-1 receptor-deficient mice, Science, 291 (2001) 319-322.

[21] A.-A. Hoseini, S. Farhadi, A. Zabardasti, F. Siadatnasab, A novel n-type CdS nanorods/p-type LaFeO3 heterojunction nanocomposite with enhanced visible-light photocatalytic performance, RSC Advances, 9 (2019) 24489-24504.